The use of solar radiation models to derive atmospheric turbidity: an inter-comparison study

Omar Behar[1,2], Daniel Sbarbaro[1,2], Aitor Marzo[3,4], M. Trigo Gonzalez[3,4], E. Fuentealba Vidal[3,4], Luis Moran[1,2]

[1] Solar Energy Research Center (SERC-Chile), Av. Tupper 2007 Piso 4, Santiago, Metropolitan Region (Chile).

[2] Faculty of Engineering, University of Concepcion, Víctor Lamas 1290, Concepción, Bío Bío (Chile).

[3] University of Antofagasta, Antofagasta, Avenue Angamos 601, Antofagasta (Chile).

[4] Antofagasta Energy Development Center (CDEA-UA), Antofagasta (Chile).

Abstract

This study inter-compares the most important retrieval methods that derive atmospheric turbidity from measured Direct Normal Irradiance. A number of parametric solar radiation models are used backward to estimate the atmospheric turbidity indices. To reduce error propagation, each turbidity index are derived using a specific set of models. Then, an inter-comparison between all the selected models are carried out to establish degree of agreement between the models. High-resolution solar radiation data, at one-minute intervals, taken from Plataforma Solar del Desierto de Atacama, is used in this investigation.

Results shows that seven models (among 11 models) generally agree well, with a maximum difference of 0.004 in the estimation of the Angstrom coefficient. Besides, Kasten's pyrheliometric method performs as good as sophisticated solar radiation models such as METSTAT, MWLT1, MWLT2, REST and Yang.

Keywords: Atmospheric turbidity, Linke turbidity factor, AOD, Angstrom coefficient, retrieval method.

1. Introduction

The evaluation of atmospheric turbidity from measured solar radiation has been widely used as an alternative to complex and expensive instruments. Indeed, the convenient turbidity indices are Angstrom turbidity coefficient (β), Linke turbidity factor (TL), and Aerosols Optical Depth (AOD) (Yousef et al. 2012).

To retrieve atmospheric turbidity from solar irradiance data, previous studies have frequently used Kasten's and Louche's methods to determine TL and β, respectively. Based on these retrieval methods, Chaâbane (2008) has investigated the daily and monthly variations of TL and β, at two different sites, in Tunisia. Dos Santos and Escobedo (2016) have estimated the hourly and monthly average values of TL over São Paulo, Brazil. Chaiwiwatworakul and Chirarattananon (2004) have used radiation measurements to evaluate the atmospheric turbidity at Bankok. Ellouz et al. (2013) have used Kasten's pyrheliometric formula to derive TL over Sidi Bou Said, Tunisia. Marif et al. (2019) have used Kasten's and Dogniaux's methods to estimate the mean TL and β over Adrar, Algeria. Zakeya et al. (2004) have used hourly measurements of Direct Normal Irradiance (DNI) at Aswan and Cairo, Egypt, to estimate AOD, TL, and β.

Recently, Gueymard (2013) has investigated the potential of parametric solar radiation models to derive AOD from irradiance measurements. The performance of seven models, including REST2, CPCR2, MLWT1, MLWT2, REST, Louche and METSTAT have been examined, under the US climate.

The objective of the present study is the inter-comparison of the most important retrieval methods that derive atmospheric turbidity indices from measured DNI to establish their degree of agreement and to examine the potential of Kasten's pyrheliometric formula against high-performance radiation models. Various parametric solar radiation models, which evaluate solar irradiance as a function of atmospheric parameters, are used backward to derive turbidity indices including AOD, TL and β. As the first step, each turbidity index is derived using a specific set of models. After that, an inter-comparison between all the models is carried out. Northern Chile was selected to carry out this investigation. The next section highlights the methodology used to derive turbidity indices.

doi:10.18086/swc.2019.42.02 Available at http://proceedings.ises.org

Section 3 describes the solar radiation data and the models' inputs. The results are discussed in section 4 and the conclusions are summarized in the last section.

2. Methodology

Retrieval methods are an inverse technique that derive turbidity from measured solar irradiance. For each turbidity index, a set of radiation models is sued with the aim to reduce error propagation. The selection criteria are the model's inputs. Some models require broadband turbidity information and thus they are more suitable to derive TL and AOD. However, other solar radiation models need spectral information, therefore, they are more appropriate to determine β.

The approach used herein to get the atmospheric turbidity consists in the use of an iterative process to find the turbidity parameters that match the estimated and measured DNI values. The following sections highlight the selected models to derive turbidity.

2.1. Derivation of the Linke turbidity factor

Typical solar radiation model that predicts DNI as a function of TL has the following form:

$$G_b = E_{ex}\exp(-M\delta_{cda}TL) \quad \text{(eq. 1)}$$

Where: E_{ex} is the extraterrestrial radiation, δ_{cad} is the clean-dry atmosphere optical depth, M is the air mass and TL is the Linke turbidity factor.

Three solar radiation models namely Ineichen (Ineichen and Perez, 2002), ESRA (Gueymard, 2012) and Molineaux (Molineaux et al., 1998) are used to determine TL. In addition to these models, Kasten's pyrheliometric method (Kasten, 1980) is also considered.

2.2. Derivation of the aerosols optical depth and the Angstrom turbidity coefficient

The most appropriate solar radiation models to derive AOD and β from measured DNI have the following form:

$$G_b = E_{ex}\prod_{i=1}^{n}\tau_i \quad \text{(eq. 2)}$$

Where: τi is the scattering -transmittances of the individual extinction processes (i).

Indeed, solar radiation models use different approaches to estimate aerosols scattering -transmittance. The AOD could be derived from the models that estimate aerosols scattering-transmittance (τ_a) based on Bouguer-Lambert-Beer's law:

$$\tau_a = \exp(-M_a AOD) \quad \text{(eq. 3)}$$

Where: subscript "a" refers to aerosols.

Two solar radiation models "METSTAT (Maxwell, 1998) and CEM (Atwater and Ball, 1978)" and the method proposed by Gueymard (Gueymard, 1998) are considered to estimate the AOD.

To determine β, four high-performance parametric models that require spectral turbidity information are used: MWLT1 (Gueymard, 1998), MLWT2 (Gueymard, 2003), REST (Gueymard, 2003), and Yang (Yang et al., 2001).

3. Solar radiation data and models' inputs

High resolution (one-minute intervals) radiometric and climate data have been taken from the radiometric station, Plataforma Solar del Desierto de Atacama (PSDA), which belongs to and is managed by the Centro de Desarrollo Energético Antofagasta (CDEA) of the University of Antofagasta (UA). It is located in the north of Chile (Latitude: 69,929 S, Longitude: 24,090 W, Elevation: 965 m). PSDA The measured data used in this study (from 1 January to 31 March 2018) includes ambient temperature, relative humidity, atmospheric pressure, wind speed and DNI. Since some of the models' inputs were not measured during the selected, the following data are used:

- The ozone amount has been estimated using Van Heuklon's model (Van Heuklon, 1997),

- The amount of nitrogen dioxide have defaulted to 0.204 matm-cm,

- Reanalysis data of Precipitable Water (PW) and Angstrom exponent (α) have been taken from NASA's Modern-

Era Retrospective analysis for Research and Applications (MERRA) (https://giovanni.gsfc.nasa.gov/giovanni/). The potential of MERRA's reanalysis data are already proven in previously published works (Gueymard, 2013, 2014). MERRA provides gridded data at hourly intervals with a 0.67° x 0.5° spatial resolution. For this reason, time area-averaged interpolation are used to get one-minute interval data. For the case of measured DNI, Ineichen's method (Ineichen, 2006) is applied to identify clear sky data to meet the requirements of retrieval methods (Gueymard, 2013). Aa a result, 12724 data are considered in the present investigation. Figure1 (left) illustrates the filtered clear sky DNI data while Figure 1 (right) shows the hourly MERRA's PW data observed on January 21, 2018.

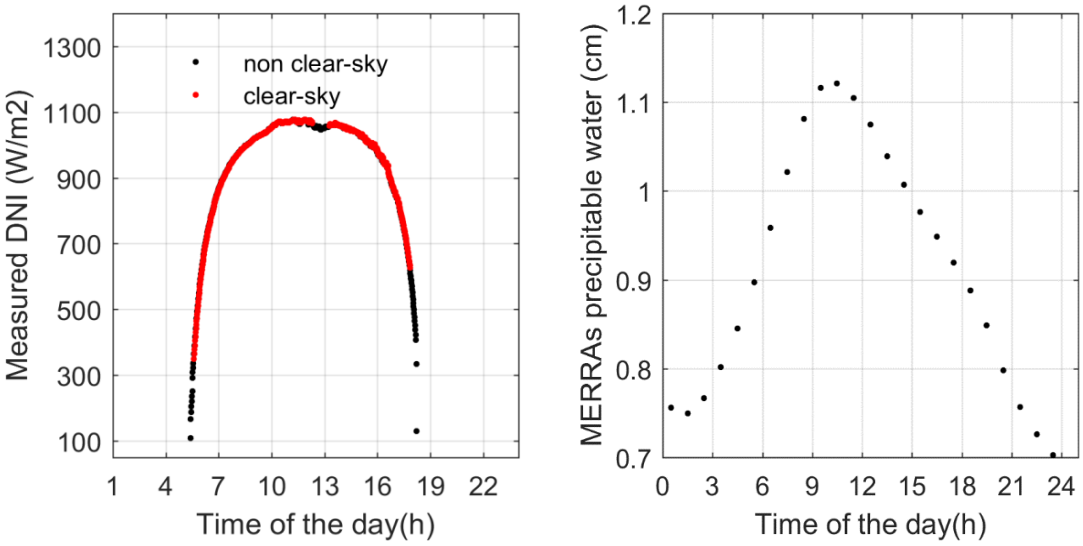

Fig. 1: Clear-sky DNI data selection (left) and MERRA's PW data (right) during January 21, 2018

4. Results and discussion

In this section, the derived turbidity indices from the above-cited models are discussed. In the first step, the models that belong to the same set are compared to each other to examine their potentials to derive specific turbidity index. Then, an inter-comparison between all the models is carried out to establish the degree of agreement between the models in the prediction of atmospheric turbidity and to examine the potential of Kasten's formula.

4.1. Aerosol Optical Depth

Figure 2 shows the diurnal and the monthly variations of the derived ADO for a 3-months period in 2018, using Gueymard, METSTAT, and CEM models. METSTAT and Gueymard agree generally well with occasional minor differences at low aerosols turbidity (low values of AOD). CEM seems to overestimate AOD at a high atmosphere's turbidity (compared with METSTAT and Gueymard's method).

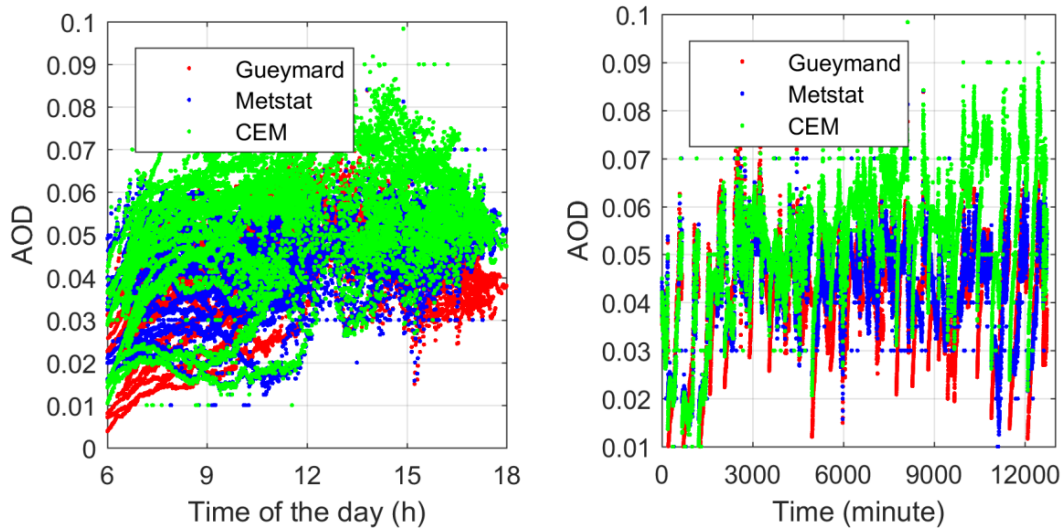

Fig. 2: Variations of the modeled AOD at PSDA, Chile, January-March 2018 using three different models. Diurnal variation (left) and monthly variation (right).

Figure 3 illustrates an inter-comparison between the AOD-derived models. It is apparent that Gueymard model agrees well with METSTAT. Table 1 illustrates the statistics of each model. Overall, the CEM model provides the highest AOD values, whereas Gueymard's AOD values are the lowest. Besides, METSTAT has the lowest standard deviation.

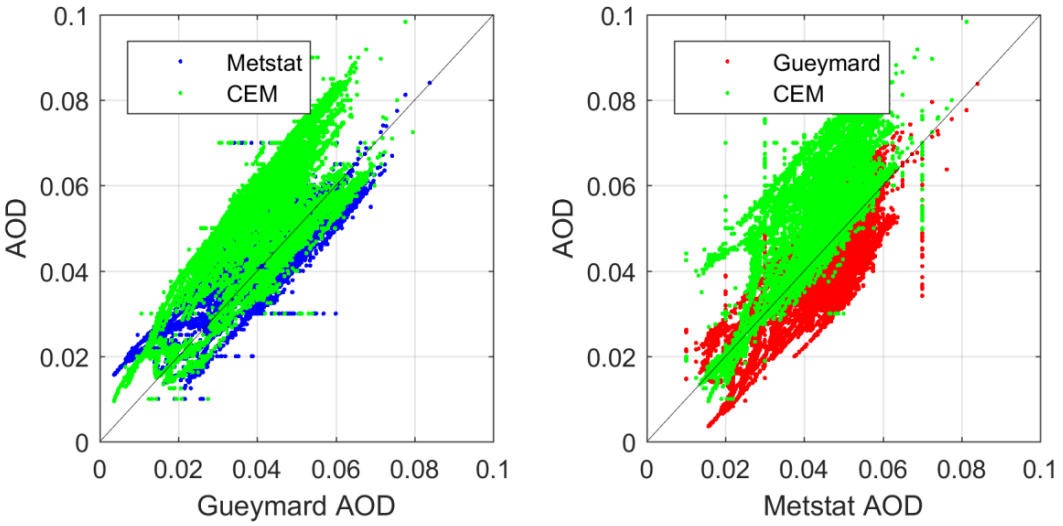

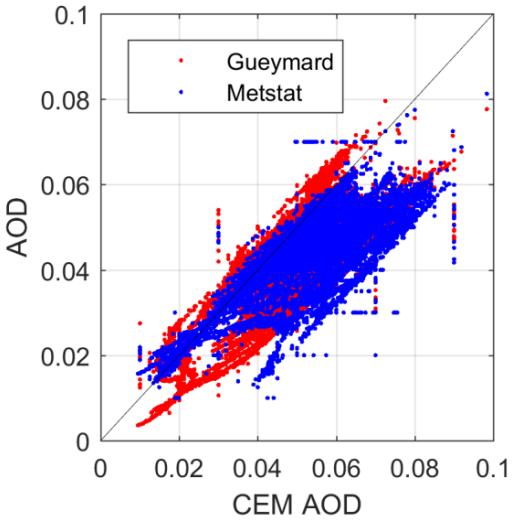

Fig. 3: Inter-comparison of AOD-derived models

Tab. 1: Statistics of the derived turbidity information

Turbidity index	Statistics	Max	Mean	Std
AOD	Gueymard	0.0838	0.0411	0.0116
	METSTAT	0.0841	0.0430	0.0104
	CEM	0.1041	0.0526	0.0143
TL	Kasten	3.20	2.15	0.15
	Ineichen	3.84	2.39	0.13
	ESRA	3.33	2.23	0.17
	Molineaux	3.08	2.05	0.13
β	MWLT1	0.0520	0.0259	0.0070
	MWLT2	0.0518	0.0250	0.0074
	REST	0.0416	0.0227	0.0061
	Yang	0.0484	0.0231	0.0064

4.2. Linke turbidity factor

Figure 4 illustrates the diurnal and the monthly variations of the derived TL using four models: Kasten, Ineichen, ESRA, and Molineaux. There is a significant difference between the models. Indeed, the value of TL is strongly related to the expression used to estimate the optical thickness of the Clean-Dry-Atmosphere (δ_{cda}) [22]. The four considered models use different expressions to estimate δ_{cda}, which results in different values of TL. Interestingly, this results in a minor difference in the mean values of TL, as highlighted in Table 1.

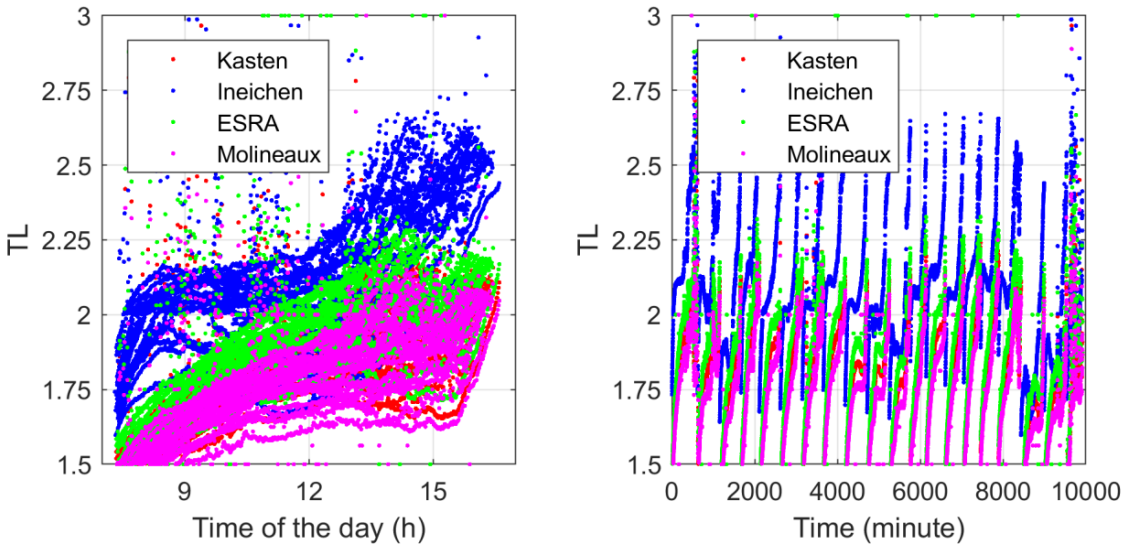

Fig. 4: Derived TL at PSDA, Chile, January-March 2018 using four different models. Diurnal variation (left) and monthly variation (right)

Figure 5 illustrates an inter-comparison between the TL-derived models. Kasten, ESRA, and Molineaux follow a similar temporal pattern. In fact, the definition of TL for these models depends on the air mass (Ineichen and Perez, 2002), which in its turn depends on solar elevation (see Figure 4, right). Ineichen's model uses air-mass-independent TL (Ineichen and Perez, 2002), thus, it provides different values compared to the three other models. Overall, Ineichen provides the highest values of TL (blue color in Figure 5), whereas Molineaux's values (margarita color) are the lowest.

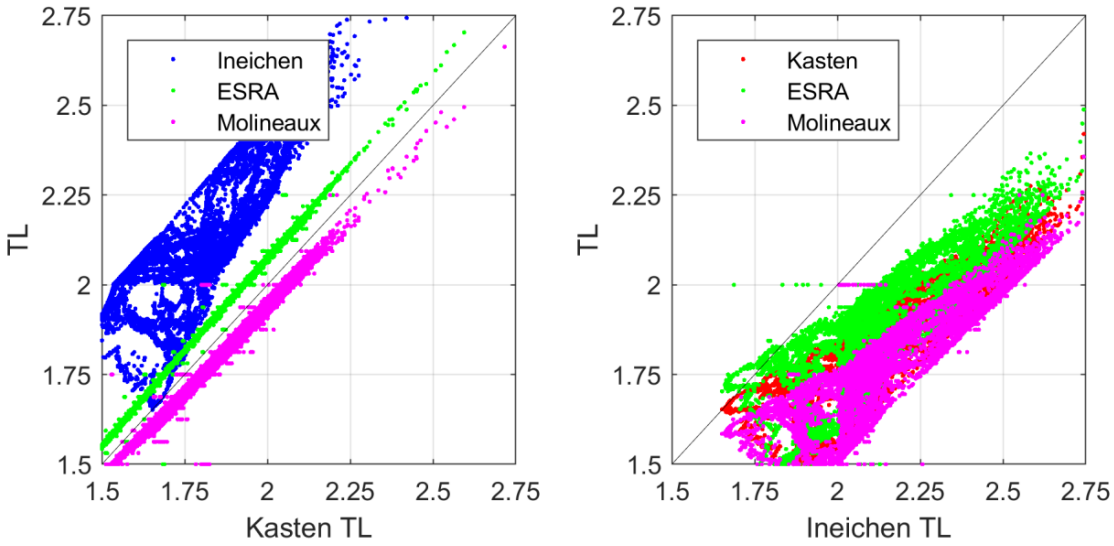

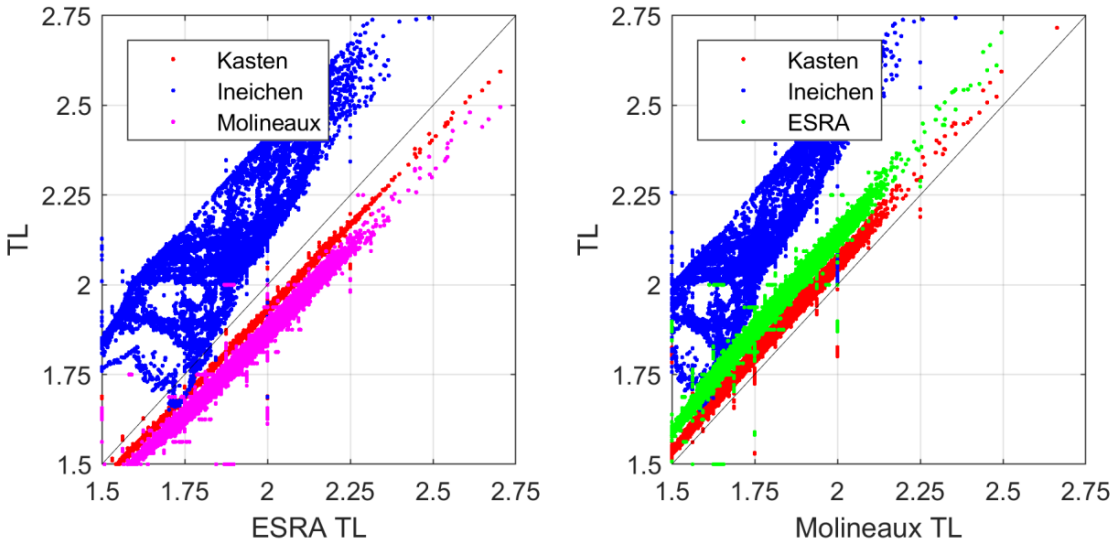

Fig. 5: Inter-comparison of Linke-derived models

4.3. Angstrom turbidity coefficient

Figure 6 shows diurnal and monthly variations of the derived β during a 3-months period. Four high-performance solar radiation models are used to derive β from measured data of DNI: MWLT1, MWLT2, REST, and Yang. Indeed, β is the most important turbidity index and it represents the amount of aerosols in the atmosphere (Jacovides, 1997). The results indicated that PSDA is a low-turbidity region, which shows that Chilean Atacama is very promising for solar energy applications (at least around PSDA). As illustrated in Table 1, the mean values of β ranges from 0.0227 to 0.0259, depending on the derived-model. The maximum value of β is 0.052, a value that is so much lower than those measured at the MENA region (Gueymard, 2012).

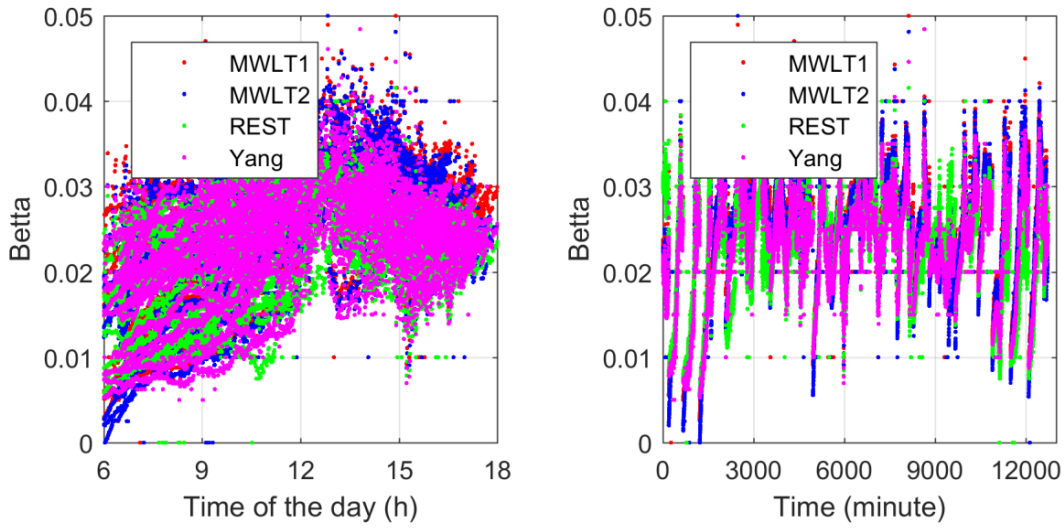

Fig. 6: Variations of derived β at PSDA, Chile, during January-March 2018 using four different models. Diurnal variation (left) and monthly variation (right)

Figure 7 illustrates an inter-comparison between the derived βs using four different models. It can be observed that MWLT1, MWL2, and Yang agree generally well, with a slight difference at low aerosols turbidity. REST seems to underestimate β (compared to the three other models). However, the four models provide almost the same mean β (see Table 1).

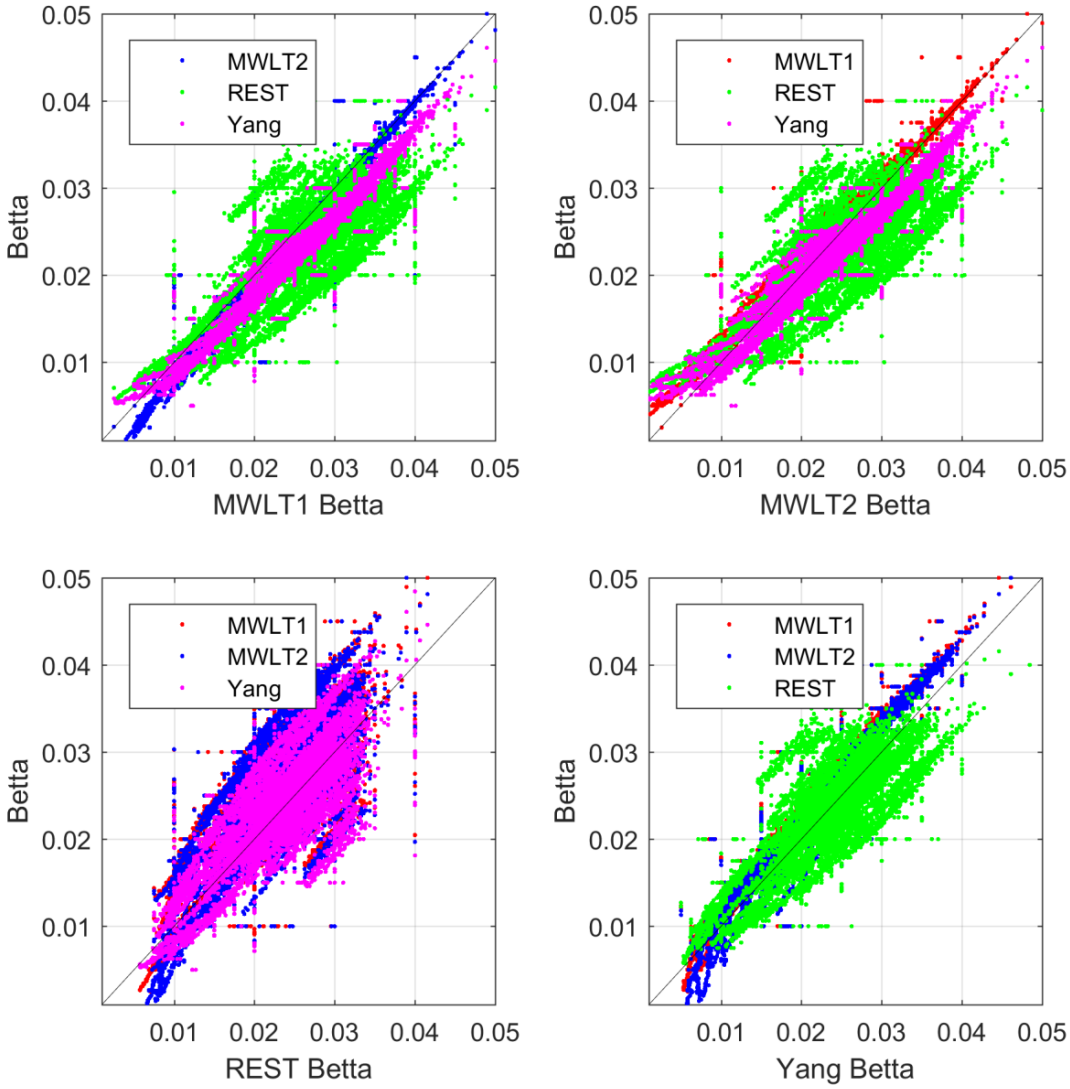

Fig. 7: Inter-comparison of β-derived models

5. Inter-comparison of the models to predict the Angstrom turbidity coefficient

This section aims to assess the degree of agreement between the all considered models in this study. For the case of Linke-dependent models, β is extracted from TL using expression of Remund et al. (2003):

$$\beta = \left[\frac{TL}{0.8662} - (1.8494 + 0.2425\mathrm{PW} - 0.0203\mathrm{PW}^2)\right] \quad \text{(eq. 4)}$$

Where: PW is the amount of precipitable water in the atmosphere.

For the case of AOD-dependent models, Angstrom's law is used to derived β from AOD:

$$AOD_\lambda = \beta\lambda^{-\alpha} \quad \text{(eq. 5)}$$

The results are highlighted in Table 2. It is apparent that the use of mathematical relations to derive turbidity parameters from each other is an efficient technique. A good agreement between seven models (among 11 models) has been observed. The maximum difference of less than 0.004 in the prediction of β is obtained between Mestat and REST.

Tab. 2: Inter-comparison of 11 models to derive Angstrom turbidity coefficient

Set of models	Statistics	Max.	Mean	Std.

AOD-dependent models	Gueymard	0.0494	0.0253	0.0069
	METSTAT	0.0496	0.0265	0.0061
	CEM	0.0614	0.0324	0.0086
TL-dependent models	Kasten ajusted	0.0565	0.0254	0.0113
	Ineichen	0.0770	0.0435	0.0095
	ESRA	0.0928	0.0315	0.0123
	Molineaux	0.0933	0.0184	0.0098
B-dependent models	MWLT1	0.0520	0.0259	0.0070
	MWLT2	0.0518	0.0250	0.0074
	REST	0.0416	0.0227	0.0061
	Yang	0.0484	0.0231	0.0064

Interestingly, Kasten's method has shown good agreement with high-performance solar radiation models, such as MLWT1, MWLT2, and Yang. The difference in the estimation of β between Kasten's method and MLWTs is less than 0.0005, which is negligible. It also agrees well with AOD-dependent models, particularly METSTAT (a model developed by the US NREL).

Figure 8 shows an inter-comparison between Kasten's method, METSTAT, and four β-dependent models. Good agreement is obtained, particularly at moderate aerosols turbidity. Therefore, the use of Kasten's method to derive TL and then extracte β and OAD from TL using mathematical expressions "eqs. 4 and 5" is an efficient methodology to estimate the atmospheric turbidity. The advantage of such a methodology is that does not need any atmospheric data except PW. Only two measured data are needed namely DNI and PW, which will not induce a significant error propagation in the estimation of the atmospheric turbidity. Nevertheless, this recommendation does not discount the potential of high-performance radiation models, which could be more accurate when detailed data about the atmosphere is available.

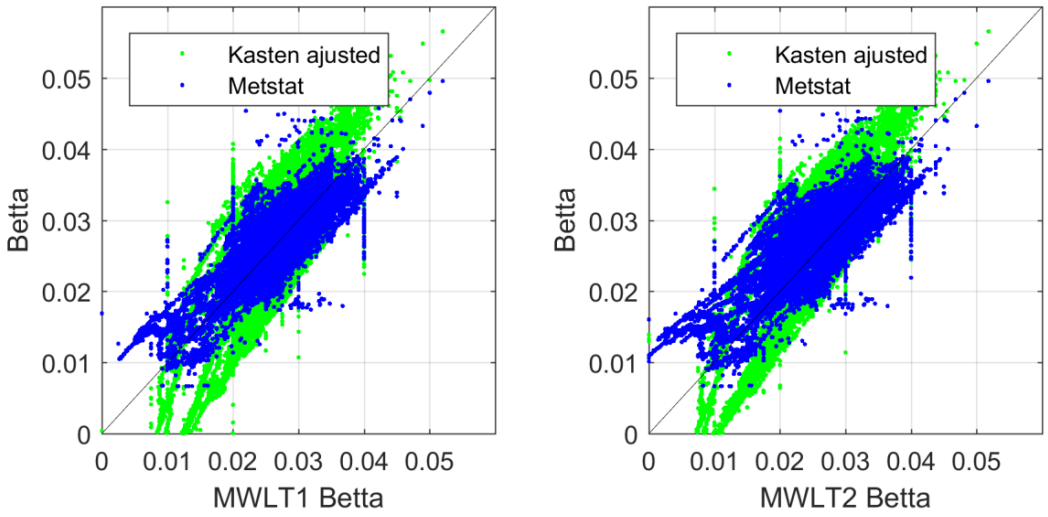

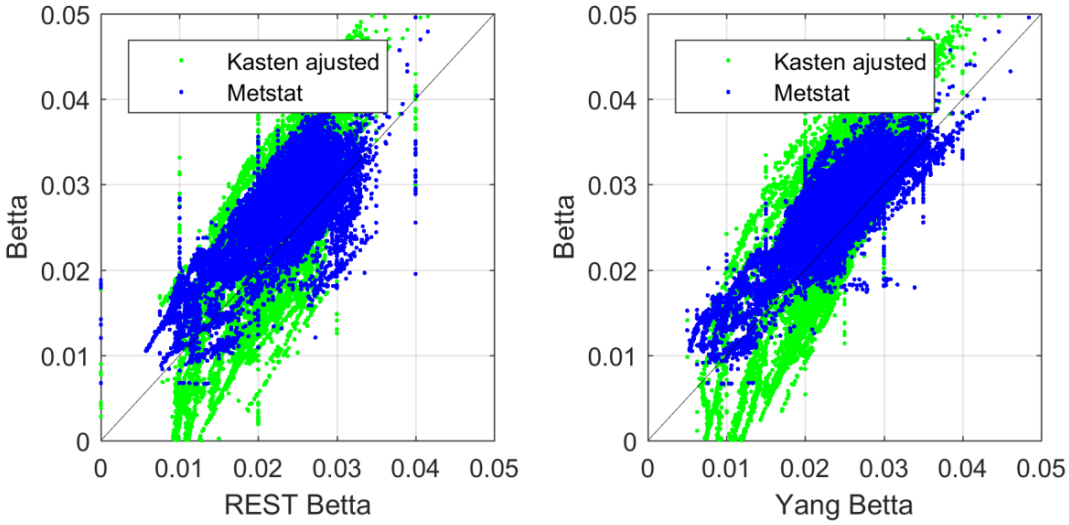

Fig. 8: Density plots of Kasten's method and METSTAT model vs. high-performance solar radiation models

6. Conclusion

A comprehensive inter-comparison of the most important retrieval methods that derive atmospheric turbidity from measured DNI is presented in this paper. Eleven models are used to derive three turbidity indices namely: TL, β, and OAD. The study focused on the Chile's Atacama, a region that is rarely considered in previously published studies. A number of parametric solar radiation models were used backward to derive atmospheric turbidity. To reduce error propagation, each turbidity index was derived using a specific models. For the case of the AOD, METSTAT, and CEM in addition to the method proposed by Gueymard are employed. METSTAT and Gueymard showed a good agreement, while CEM relatively overestimates the AOD. To determine TL, three solar radiation models namely Ineichen, ESRA, and Molineaux were used and particular attention has been given to Kasten's method. A remarkable difference between TL-dependent models was observed. Indeed, Kasten, ESRA, and Molineaux are air-mass-dependent and thus they provide a similar temporal pattern. For the case of β, four high-performance parametric models are used: MWLT1, MLWT, REST, and Yang. These models agree generally well with a slight difference at low aerosols turbidity.

To examine the degree of agreement between the 11 selected models in this study, β was extracted from from TL-dependent and AOD-dependent models using simple expressions. The study concludes that the use of mathematical relations to derive turbidity parameters from each other is an efficient technique. Good agreement between seven models was observed with a maximum difference of less than 0.004 between Mestat and REST.

Particular interest was given to Kasten's method with the goal to select a simple-efficient methodology to determine turbidity from minimum measured parameters. Remarkably, the method has shown good agreement with high-performance solar radiations models such as MLWTs with a difference of less than 0.0005 in the estimation of β. Moreover, it performs similar or better than METSTAT.

Some practical information was also obtained through the present analysis. Indeed, PSDA has shown low-turbidity. Overall, β values are around 0.025, which is lower than the values measured in the MENA region.

7. Acknowledgments

This work was supported by the Innova Chile CORFO, PROJECT CODE: 17BPE3-83761, CONICYT/FONDAP/ 15110019 "Solar Energy Research Center" SERC-Chile, and the Chilean Economic Development Agency (CORFO) with contract No 17PTECES-75830 under the framework of the project "AtaMoS TeC".

We acknowledge the maintenance staff and researchers from PSDA and CDEA-UA.

8. References

Atwater, M.A., Ball, J.T., 1978. A numerical solar radiation model based on standard meteorological observations. Solar Energy 21, 163–170.

Chaâbane M., 2008. Analysis of the atmospheric turbidity levels at two Tunisian sites. Atmospheric Research 87, 136–146.

Chaiwiwatworakul P., Chirarattananon S., 2004. An investigation of atmospheric turbidity of Thai sky. Energy and Buildings 36, 650–659.

Dos Santos, C. M., Escobedo J., F., 2016. Temporal variability of atmospheric turbidity and DNI attenuation in the sugarcane region, Botucatu/São Paulo/Brazil. Atmospheric Research 181, 312–321.

Ellouz F., Masmoudi M., Medhioub K., 2013. Study of the atmospheric turbidity over Northern Tunisia. Renewable Energy 51, 513–517.

Gueymard C. A., 1998. Turbidity Determination from Broadband Irradiance Measurements: A Detailed Multicoefficient Approach. Journal of applied meteorology 37, 414-435.

Gueymard C.A., 2003. Direct solar transmittance and irradiance predictions with broadband models. Solar Energy. 74, 355-395.

Gueymard C., A., 2012. Clear-sky irradiance predictions for solar resource mapping and large-scale applications: Improved validation methodology and detailed performance analysis of 18 broadband radiative models. Solar Energy 86, 2145–2169.

Gueymard C. A., 2013. Aerosol turbidity derivation from broadband irradiance measurements: methodological advances and uncertainty analysis. ASES Solar Conf., Baltimore, MD.

Gueymard C. A., 2014. Impact of on-site atmospheric water vapor estimation methods on the accuracy of local solar irradiance predictions. Solar Energy 101, 74–82.

Ineichen P., Perez R., 2002. A new air mass independent formulation for the Linke turbidity coefficient. Solar energy 73, 151–157.

Ineichen P., 2006. Comparison of eight clear sky broadband models against 16 independent data banks. Solar Energy 80, 468–478.

Jacovides C. P., 1997. Model comparison for the calculation of linke's turbidity factor. International journal of climatology 17, 551–563.

Kasten, F., 1980. A simple parameterization of two pyrheliometric formulae for determining the Linke turbidity factor. Meteorol. Rundsch. 33, 124–127.

Marif Y., Bechki D., Zerrouki M., Belhadj M., Bouguettaia H., Benmoussa H., 2019. Estimation of atmospheric turbidity over Adrar city in Algeria. Journal of King Saud University – Science Journal of King Saud University – Science 31, 143–149.

Maxwell, E.L., 1998. METSTAT—The solar radiation model used in the production of the National Solar Radiation Data Base (NSRDB). Solar Energy 62, 263–279.

Molineaux, B., Ineichen, P., O'Neil, N., 1998. Equivalence of pyrheliometric and monochromatic aerosol optical depths at a single key wavelength. Appl. Opt. 37, 7008–7018.

NASA's Modern-Era Retrospective analysis for Research and Applications (MERRA). https://giovanni.gsfc.nasa.gov/giovanni/

Remund J., Wald L., Lefevre M., Ranchin T., Page J., 2003. Worldwide Linke turbidity information. Proceedings of ISES Solar World Congress, 16-19 June, Stockholm, Sweden.

Van Heuklon T. K., 1997. Estimating atmospheric ozone for solar radiation models. Solar energy 22, 63-68.

Yang K., Huang G.W., Tamai N., 2001. A hybrid model for estimating global solar radiation. Solar Energy 70, 13–22.

Yousef A. Eltbaakh, M.H. Ruslan, M.A. Alghoul, M.Y. Othman, K., 2012. Sopian. Issues concerning atmospheric turbidity indices. Renewable and Sustainable Energy Reviews 16, 6285–6294.

Zakeya A. S., Abdelwahab M.M., Makar P.A., 2004. Atmospheric turbidity over Egypt. Atmospheric Environment 38, 1579–1591.